



POLİTEKNİK DERGİSİ

*JOURNAL of POLYTECHNIC*

ISSN: 1302-0900 (PRINT), ISSN: 2147-9429 (ONLINE)

URL: <http://dergipark.org.tr/politeknik>



**Depolama tanklarının imalatında farklı amperlerde tozaltı kaynağının uygulanması ve kaynak bölgesinin incelenmesi**

*Application of submerged arc welding at different amperages in the manufacture of storage tanks and examination of the weld zone*

**Yazar(lar) (Author(s)):** Yiğitcan ATILGAN<sup>1</sup>, Mehmet Serkan YILDIRIM<sup>2</sup>, Yakup KAYA<sup>3</sup>

ORCID<sup>1</sup>: 0000-0001-6244-6102

ORCID<sup>2</sup>: 0000-0001-6133-6905

ORCID<sup>3</sup>: 0000-0002-9951-2844

**To cite to this article:** Atılğan Y., Yıldırım M. S. ve Kaya Y., “Application of Submerged Arc Welding at Different Amperages in The Manufacture of Storage Tanks and Examination of the Weld Zone”, *Journal of Polytechnic*, \*(\*) : \*, (\*).

**Bu makaleye şu şekilde atıfta bulunabilirsiniz:** Atılğan Y., Yıldırım M. S. ve Kaya Y., “Depolama Tanklarının İmalatında Farklı Amperlerde Tozaltı Kaynağının Uygulanması ve Kaynak Bölgesinin İncelenmesi”, *Politeknik Dergisi*, \*(\*) : \*, (\*).

**Erişim linki (To link to this article):** <http://dergipark.org.tr/politeknik/archive>

**DOI:** 10.2339/politeknik.1399878

# Application of Submerged Arc Welding at Different Amperages in The Manufacture of Storage Tanks and Examination of the Weld Zone

## Highlights

- ❖ Submerged arc welding application using different amperage values of ASTM A36 steels.
- ❖ Investigating the effect of different amperage values with destructive and non-destructive testing methods.

## Graphical Abstract

ASTM A36 steel plates are joined by submerged arc welding method using different amperage values.

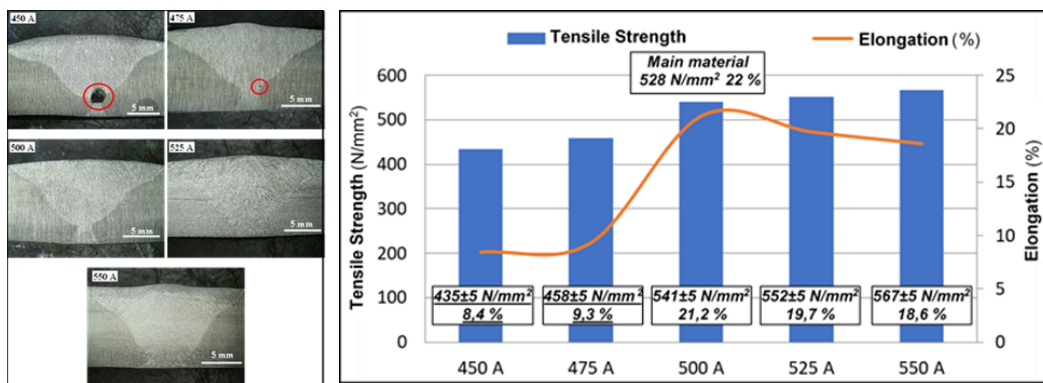


Figure. Macrostructure images and tensile/elongation graph

## Aim

Investigation of welding of ASTM A36 steels.

## Design & Methodology

Joining ASTM A36 steels by submerged arc welding using values of 450 A, 475 A, 500 A, 525 A and 550 A.

## Originality

Both non-destructive and destructive tests were performed on ASTM A36 steels joined by submerged arc welding using different amperage values.

## Findings

As a result of destructive and non-destructive tests, it was determined that there were various welding defects in welded joints at 450 A and 475 A.

## Conclusion

It has been determined that ASTM A36 steels can be joined by submerged arc welding using values of 500 A, 525 A and 550 A.

## Declaration of Ethical Standards

The author(s) of this article declare that the materials and methods used in this study do not require ethical committee permission and/or legal-special permission.

# Application of Submerged Arc Welding at Different Amperages in the Manufacture of Storage Tanks and Examination of the Weld Zone

*Araştırma Makalesi / Research Article*

Yiğitcan ATILGAN<sup>1</sup>, Mehmet Serkan YILDIRIM<sup>2</sup>, Yakup KAYA<sup>1\*</sup>

<sup>1</sup>Teknoloji Fakültesi, İmalat Mühendisliği Bölümü, Karabük Üniversitesi, Türkiye

<sup>2</sup> Teknik Bilimler MYO, Makine ve Metal Teknolojileri Bölümü, Gazi Üniversitesi, Türkiye

(Geliş/Received : 04.12.2023 ; Kabul/Accepted : 30.01.2024 ; Erken Görünüm/Early View : 15.02.2024 )

## ABSTRACT

In the study, ASTM A36 steel materials were combined with submerged arc welding using different amperages. Non-destructive magnetic particle (MT), liquid penetrant (SP), radiographic (RT), and ultrasonic (UT) examinations were performed on the joints. In addition, optical microscope, microhardness, bending, tensile, and notch impact tests were carried out on the welds. As a result of the RT and UT examinations, a lack of root penetration was found in the welds made at 450 A and 475 A. In the optical microscope examinations, the areas formed by the HAZ-weld metal transition were found to have a similar appearance for each amperage. In the microhardness studies, the hardness values are listed as weld metal, HAZ, and base material from high to low. From the notch impact tests, it was found that increasing the temperature increased the toughness value. From the bending tests performed on the joints where 450A and 475A were used, it was found that cracks and tears occurred. In addition, a rupture occurred in the weld metal during the tensile tests conducted on the joints made at 450 A and 475 A. For the joints made at other amperage values, it occurred in the base material.

**Keywords:** ASTM A36 steel, different amperage values, submerged arc welding, mechanical test.

## Depolama Tanklarının İmalatında Farklı Amperlerde Tozaltı Kaynağının Uygulanması ve Kaynak Bölgesinin İncelenmesi

öz

Bu çalışmada, 10 mm kalınlığındaki ASTM A36 çeliği tozaltı ark kaynak yöntemiyle birleştirilmiştir. Farklı kaynak akımlarının kaynak bölgesine etkisi, tahribatsız ve tahribatlı muayene yöntemleriyle incelenmiştir. Kaynaklı birleştirmelerin tahribatsız incelemelerinde sıvı penetrant (SP), manyetik parçacık (MT), ultrasonik (UT) ve radyografik (RT) muayene yöntemleri kullanılmıştır. Kaynaklı birleştirmelerin makro-mikroyapı ve mekanik özelliklerini belirlemek için ise tahribatlı muayene yöntemlerinden optik mikroskop, mikrosertlik çalışmaları, çekme, eğme ve çentik darbe testleri uygulanmıştır. Tahribatsız muayene yöntemleri sonucunda; SP ve MT yöntemlerinde kaynak yüzeyinde herhangi bir süreksizliğe rastlanmamıştır. UT ve RT incelemelerinde ise 450 A ve 475 A kaynak akımında birleştirilen levhalarda kök nüfuziyet eksikliği gözlemlenmiştir. Tahribatlı muayene yöntemleri sonucunda; makroyapı incelemelerinde, 450 A ve 475 A kaynak akımlarında birleştirilen levhaların kök kaynaklarında eksik nüfuziyet gözlemlenmiştir. Mikroyapı incelemelerinde, kaynak metali-ITAB geçiş bölgelerinin birbirlerine benzer görüntüler sergilediği belirlenmiştir. Sertlik testlerinde sonucunda en yüksek sertlik değerleri, kaynak metalinden elde edilirken onu sırasıyla ITAB ve ana malzeme takip etmiştir. Çentik darbe test sonuçları incelendiğinde, sıcaklık yükseldikçe tokluk değerlerinin arttığı tespit edilmiştir. Eğme testleri sonucunda, 450 A ve 475 A kaynak akımlarında birleştirilen levhalarda yırtılma ve çatlak tespit edilmiştir. Çekme testleri sonucunda, 450 A ve 475 A kaynak akımlarında birleştirilen levhalarda kopma kaynak metalinde gerçekleşmiş diğer kaynak akımlarında ise kopma ana malzemede gerçekleşmiştir.

**Anahtar Kelimeler:** ASTM A36 çeliği, farklı amper değerleri, tozaltı ark kaynağı, mekanik test.

### 1. INTRODUCTION

Steel consumption in the manufacture of storage tanks is quite high. In particular, tanks are manufactured from flat or bent plates. In recent years, the use of high-strength fine-grained steels and light alloys has increased in order to

extend the service life of storage tanks. However, the production costs of many materials and the need for low carbon steel for mass production should not be ignored [1].

ASTM A36 steels; It is widely used in construction machinery manufacturing, construction equipment manufacturing, general structural plates, various machine parts manufacturing, railway and land vehicle manufacturing [2-4]. This frequency of use

\*Sorumlu Yazar (Corresponding Author)  
e-posta : ykaya@karabuk.edu.tr

has highlighted the need to join ASTM A36 steels by various methods. One of the most common joining methods is welding. Welding is a reliable and efficient metal joining process that is widely used in the infrastructure and heavy equipment industries, such as steel bridge construction, shipbuilding and the installation of large pipelines [3-6]. High joint efficiency, ease of installation and low manufacturing costs are the advantages of this joining process [7-11].

Submerged arc welding is a fusion welding process used to produce machine parts and tools with basic surface properties such as corrosion resistance, wear resistance and pressure tightness [12]. This process has a high material deposition rate and is often suitable for working in a horizontal position. In addition, the main difference between submerged arc welding and other welding methods is that the arc is completely immersed in granular flux and is not visible. This process minimises heat loss and can achieve thermal efficiencies in excess of 90%. Weld seams produced by submerged arc welding have high strength and ductility with low hydrogen and nitrogen content. Differences in submerged arc welding parameters (welding current, voltage, wire feed speed, type of flux used and welding conditions, etc.) affect the weld quality and the heat affected zone [13].

In this study, ASTM A36 steel was joined by submerged arc welding using welding currents of 450A, 475A, 500A, 525A

and 550A. The effect of different current values on the weld zones was investigated. In experimental studies, the weld zones were examined using liquid penetrant (SP), magnetic particle (MT), ultrasonic (UT), radiographic (RT), optical microscope, microhardness studies, tensile, bending and notch impact tests.

## 2. EXPERIMENTAL STUDIES

Experimental studies were carried out on ASTM A36 steel plates with dimensions of 400x150x10 mm. The chemical content of ASTM A36 sheets, welding consumables and powders used in the welding process are given in Table 1. The mechanical properties of ASTM A36 steel are given in Table 2.

In accordance with EN ISO 15609-1, a 30° V weld groove was opened on ASTM A36 plates and fix from the rear, leaving a 1 mm gap. Prior to welding, the plates were turned upside down and the root pass was made using the electrode arc welding method. The plates, which had been cleaned, were then joined in a single pass using submerged arc welding at different current levels. The parameters used in the welding processes are given in Table 3. The sample image after welding is shown in Figure 1.

**Table 1.** Chemical content of base material, filler metal and powder (% by weight)

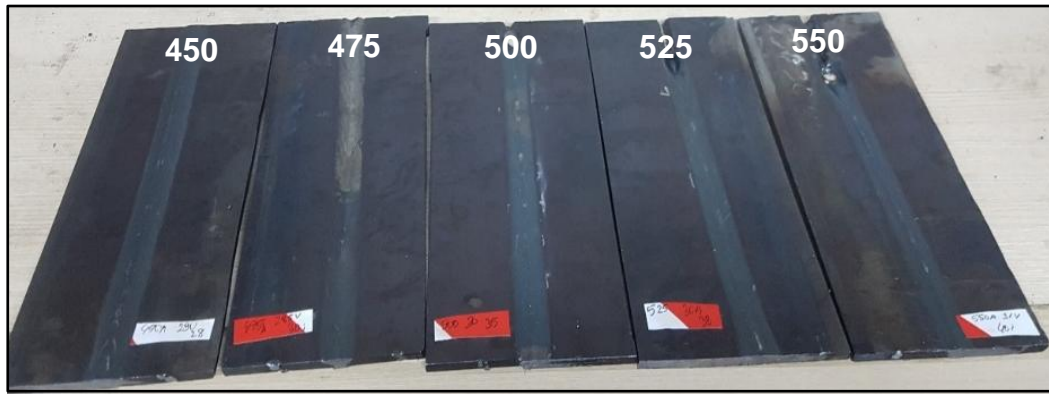
Alloying Element (%)	C	Mn	P	S	Si	Fe
ASTM A36	0,25	1	0,03	0,03	-	Balance
Filler Metal	0,04	1,3	0,025	0,02	0,25	Balance
Magma weld SF124 (powder)	0,05	1,3	0,025	0,02	0,25	Balance

**Table 2.** Mechanical properties of base material

Base Material	Yield Strength (N/mm <sup>2</sup> )	Tensile Strength (N/mm <sup>2</sup> )	Elongation (%)
ASTM A36	250	400-550	22

**Table 3.** The welding parameters

Filler Metal Diameter (mm)	Current Type	Current (A)	Volt (V)	Wire Speed (cm/min)	Heat Input (kJ/mm)
3.2	DC +	450	29	28	2,6
		475	29,5	30	2,8
		500	30	35	3
		525	30,5	38	3,2
		550	31	40	3,4



**Figure 1.** Sample image after welding

The plates joined by submerged arc welding were first subjected to non-destructive testing (NDT) by an NDT level 2 expert. BETA brand BT-68 penetrant, BT-70 developer and BT-69 cleaner were used for liquid penetrant testing. Magnetic particle testing was carried out using a Magnaflux magnetic testing device. Ultrasonic testing of the specimens was performed using a Krautkramer USM36 ultrasonic testing device with a probe at 60° and 70° angles. Radiographic testing of the plates was carried out on a Detay Quality radiographic testing machine.

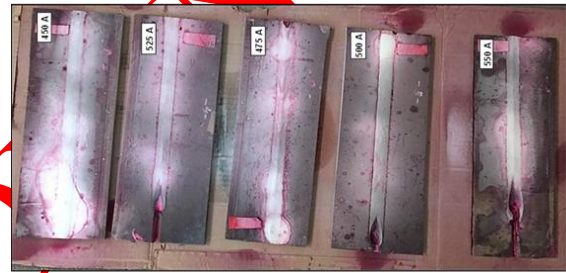
Following the application of non-destructive testing methods, the welded plates were prepared for destructive testing. Specimens were taken from the plates using a water-cooled band saw for macro/micro imaging, hardness, tensile, bending and notch impact studies. In addition, these samples were taken parallel to the rolling direction. The specimens used for macro/micro imaging were ground with sandpaper in accordance with standard metallographic specimen preparation procedures. It was polished with 3 micron diamond paste and then etched with 2% Nital solution. The microstructural studies were carried out using an Inverted Brand optical microscope. Three samples were used for each of the mechanical tests (tensile, hardness, flexural and notch) and the results were averaged over the three samples. Hardness testing was carried out using a Hardway model HV10 AP fully pneumatic variable load instrument. Vickers hardness values were used for hardness testing and a 10 kg load was applied during measurements. Tensile tests were carried out at room temperature at a tensile speed of 5 mm/min. Bending test specimens were prepared with dimensions of 130x40 mm and the mandrel diameter was determined to be 20 mm. The bending tests were performed using a Hardway/WAW 600D tensile tester at a bending speed of 10 mm/min. For the notch impact test, a 55x10x5 mm specimen of weld metal and HAZ was prepared. The notch impact tests were performed by the Charpy method using a Hardway/JB 300 B tester with a capacity of 300 joules. Tests were performed at temperatures of -20, 0 and 20 °C.

### 3. RESULTS and DISCUSSION

#### 3.1. Non-destructive Testing

##### 3.1.1 Penetrant liquid inspection

The tests were carried out by a liquid penetrant expert (Figure 2) and reported in accordance with EN ISO 23277 (Figure 3).



**Figure 2.** Liquid penetrant testing application image

When the samples were examined after the liquid penetrant test, no surface defects such as cracks, voids, pores and undercut were found on the weld surfaces. The expert's approved report stated that there were no surface defects in any of the welding currents used and that the welds were suitable. Özkan [14] stated that no discontinuity was found on the weld surface by liquid penetrant testing of structural steels after welding.

##### 3.1.2. Magnetic particle inspection

It was applied by a magnetic particle inspection test expert in accordance with the TS EN ISO 9934 standard (Figure 4) and reported in accordance with the EN ISO 23277 standard (Figure 5). Upon examination of the magnetic particle test results, no surface defects such as cracks, pores, or combustion grooves were found on the weld surfaces. In the report approved by the expert, it was determined that there were no superficial defects in all welding currents used and that the welds were in compliance with the standards. Özkan [14] reported that no cracks, pores, etc. were detected on the weld surface as a result of magnetic particle tests performed after the welding of structural steels.



<b>LIQUID PENETRANT INSPECTION</b>				Report No.	PT-001		
				Sheet/Page	1/1		
				Date	16.3.2020		
Surface Temperature : T<10 <input type="checkbox"/> 10≤T≤38 <input checked="" type="checkbox"/> T>38 <input type="checkbox"/>							
Surface Condition : AS IT IS <input checked="" type="checkbox"/> SAND BLASTED <input type="checkbox"/> GROUND <input type="checkbox"/> MACHINED <input type="checkbox"/>							
Welding Process : GTAW <input type="checkbox"/> SMAW <input type="checkbox"/> GMAW <input type="checkbox"/> SAW <input checked="" type="checkbox"/>							
Joint Type : FILLET <input type="checkbox"/> V <input checked="" type="checkbox"/> X <input type="checkbox"/> K <input type="checkbox"/> U <input type="checkbox"/>							
Penetrant Brand: BETA PROSES BT68		Dwell Time: 20 mins.		UV- Light Intensity: 500 lux			
Developer Brand: BETA PROSES BT70		Developer Time: 20 mins.					
Cleaner Brand: BETA PROSES BT69							
Sr. No	Description / Joint no	Thickness/ Length	Material Grade	Observation/ Type of Defect	Defect Location	Remarks	Result
1	<b>450 A</b>	10mm	ASTM A36				A
2	<b>475 A</b>	10mm	ASTM A36				A
3	<b>500 A</b>	10mm	ASTM A36				A
4	<b>525 A</b>	10mm	ASTM A36				A
5	<b>550 A</b>	10mm	ASTM A36				A
LEGEND for RESULT : A : Accepted R: Repair/ to be corrected							
LEGEND for TYPE OF SURFACE DEFECTS: LC: Longitudinal Crack TC: Transverse Crack CC: Crater Crack MSP: Micro Surface Porosity							
PREPARED BY (HAZIRLAYAN)				APPROVED BY (ONAYLAYAN)			
NAME: Yiğitcan ATILGAN				NAME: Kerem ÇANAKÇI			
SIGN: 				SIGN: 			
DATE: 16.03.2020				DATE: 16.03.2020			

Figure 3. Liquid penetrant inspection report



Figure 4. Magnetic particle test application image

<b>MAGNETIC PARTICLE TEST REPORT</b>		Report No.	MT-001		
		Sheet/Page	1/1		
		Date	16.3.2020		
MATERIAL THK.: 10mm					
Magnetic force application:		AC <input type="checkbox"/>	DC <input checked="" type="checkbox"/>		
Magnetic Particle Direction :		CIRCULAR <input type="checkbox"/>	LONGITUDNAL <input checked="" type="checkbox"/>		
EQUIPMENT TYPE: MAGMA FLUX					
Test Temperature: 23° C		Light Intensity: 500 lux			
Surface type:		GROUND <input type="checkbox"/>	SMOOTH <input checked="" type="checkbox"/>		
Surface condition :		WET <input type="checkbox"/>	DRY <input checked="" type="checkbox"/>		
Welding Process: SAW		Heat Treatment: Before <input type="checkbox"/> After <input type="checkbox"/> No <input checked="" type="checkbox"/>			
Joint Type: BW		Demagnetizasyon: Applied <input type="checkbox"/> Not Applied <input checked="" type="checkbox"/>			
Item No.	Weld/ Part No.	Weld/test Length	Deffect Type	Remarks	Result
1	<b>450 A</b>	400mm			A
2	<b>475 A</b>	400mm			A
3	<b>500 A</b>	400mm			A
4	<b>525 A</b>	400mm			A
5	<b>550 A</b>	400mm			A
Legend <b>A: Accepted</b> R: Repaired / to be corrected					
PREPARED BY (HAZIRLAYAN)			APPROVED BY (ONAYLAYAN)		
NAME: Yiğitcan ATILGAN			NAME: Kerem CANAKÇI		
SIGN:			SIGN:		
DATE: 16.03.2020			DATE: 16.03.2020		

Figure 5. Magnetic particle test report

### 3.1.3. Ultrasonic examination

To detect subsurface/section defects, an ultrasonic test was applied by an expert according to TS EN ISO 23279 standard (Figure 6) and reported (Figure 7).

When the ultrasonic examination results were examined, a lack of penetration at the root (insufficient penetration) was observed in processes using 450 A and 475 A welding currents. As sufficient heat input cannot be achieved at these current values (Table 3), it is thought that full penetration between the root pass and the weld (Figure 10) cannot be achieved. No discontinuities (undercut, residue, pores, cracks, etc.) were observed in the plates joined at 500 A, 525 A and 550 A. In the report approved by the expert, it was determined that the plates combined with 450 A and 475 A welding currents needed to be repaired, while the plates combined with 500 A, 525 A, and 550 A welding currents were suitable.

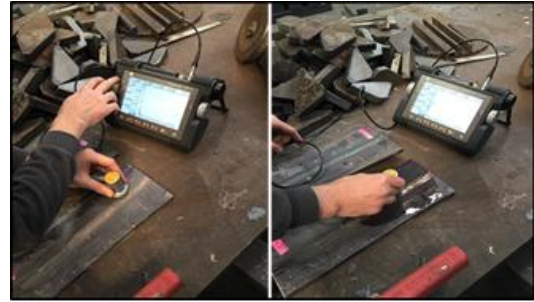


Figure 6. Ultrasonic inspection application image

As a result of ultrasonic tests applied to various steel materials joined by the submerged arc welding method, cracks, lack of penetration, gas gaps, etc. have been detected in the weld seam zone. It has been stated that no volumetric errors were encountered [14-17].


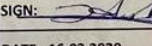
<b>ULTRASONIC INSPECTION</b>						Report No.	UT-001		
						Sheet/Page	1/1		
						Date	16.3.2020		
Weld Process		SMAW(111) <input type="checkbox"/> SAW (121) <input checked="" type="checkbox"/> GTAW (141) <input type="checkbox"/> GMAW (131/135) <input type="checkbox"/> Other							
Weld Joint Type		Butt Weld <input checked="" type="checkbox"/> Fillet Weld <input type="checkbox"/> Branch Weld <input type="checkbox"/> T-joint <input type="checkbox"/>			Joint Design V <input checked="" type="checkbox"/> X <input type="checkbox"/> U <input type="checkbox"/> K <input type="checkbox"/> Other				
Test Standard		EN ISO 17640 <input checked="" type="checkbox"/> Technique 1		ASME SEC V <input type="checkbox"/> Diğer <input type="checkbox"/>					
Evaluation Standard		EN ISO 11666 <input checked="" type="checkbox"/>		ASME ... <input type="checkbox"/> Diğer <input type="checkbox"/>					
Heat Treatment Condition		Before <input type="checkbox"/> After <input type="checkbox"/>		N/A <input checked="" type="checkbox"/>		Test Temperature 23 °C			
Material Thickness 10		Material ASTM A36							
INSTRUMENT USED		MAKE		MODEL/TYPE					
HATA DEDEKTÖRÜ		KRAUTKRAMER		USM 36					
ÖLÇÜ:	7" (Inch)	KAPASİTE:	8 GB, 3D-Kart						
ÇÖZÜNÜRLÜK:	800 x 400 piksel	DARBE:	EN 60068 Kısım 2-27 Eksen başına 1000 çevrim						
HIZ:	250 ... 16,000 m/s	KORUMA:	IP66 / IEC 60529						
PROB BAĞLANTILARI:	2 x LEMO – 1 veya 2 x BNC	ÇALIŞMA SICAKLIĞI:	-10 ...55°C						
ITEM No.	WELD No. (Part No.)	Location / Dimension of Defect				Test Length (mm)	DEFECT TYPE	DEFECT LOCATION	EVALUATION
		I1 (Q1) mm	I2 (Q2) mm	HVL mm	b (t) mm				
1	<b>450 A</b>						Db	0-30	R
2	<b>475 A</b>						C	0-30	R
3	<b>500 A</b>						C	0-30	A
4	<b>525 A</b>						C	0-30	A
5	<b>550 A</b>						C	0-30	A
EVALUATION LEGEND: <span style="border: 1px solid red; padding: 2px;">A= Acceptable</span> <span style="border: 1px solid blue; padding: 2px;">R= To be Repaired</span>									
DEFECT TYPE :									
Aa Gas cavity		Ba Slag inclusion		Db Single side root defect		Fa Excessive penetration			
Ab Elongated cavity		Bb Aligned slag inc.		Dc Incomplete penetration		Fb Imperfect shape			
Ac Aligned porosity		C Lack of fusion		E Crack		Fc Undercut			
Ad Clustered porosity		Da Root concavity		H Metallic inclusion					
PREPARED BY (HAZIRLAYAN)					APPROVED BY (ONAYLAYAN)				
NAME: Yiğitcan ATILGAN					NAME: Yiğitcan ATILGAN				
SIGN: 					SIGN: 				
DATE: 16.03.2020					DATE: 16.03.2020				

Figure 7. Ultrasonic inspection report

### 3.1.4. Radiographic examination

It was applied (Figure 8) and reported (Figure 9) by the radiographic examination specialist according to TS EN ISO 17636 standard.

When the radiographic examination results were examined, a lack of penetration into the root was observed in processes using 450 A and 475 A welding currents. No defects were found in the plates joined at 500 A, 525 A and 550 A. In the report approved by the expert, it was stated that the plates joined at 450 A and 475 A welding currents needed to be repaired. However, it has been stated that plates combined with welding

currents of 500 A, 525 A, and 550 A are suitable. Canlı [18] carried out radiographic examinations on welded connections in the production of storage tanks. Several welded joints in the storage tank exhibited pores in different directions (horizontal and vertical), slag residues in filler material, cracks caused by shrinkage in the root, and areas of insufficient penetration in some of the weld seams. It was also noted that undercut and cracks were present in the root areas of a few of the weld seams.



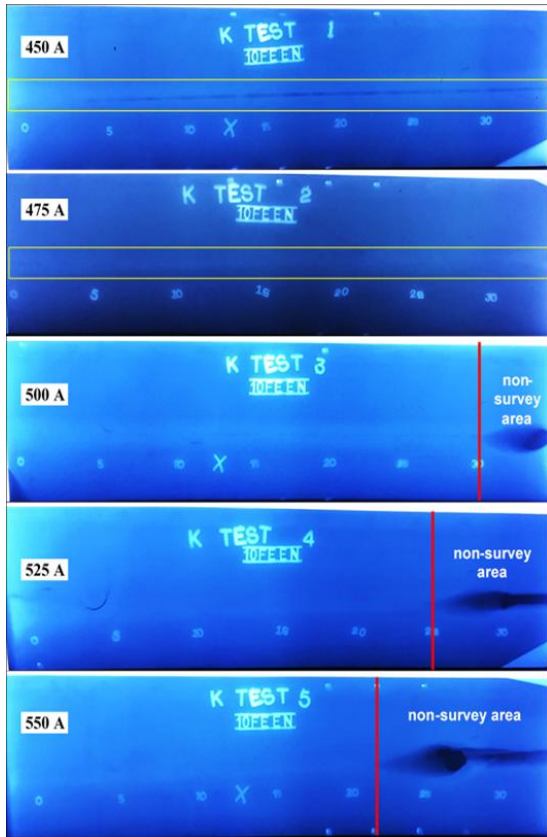


Figure 8. Radiographic examination method images

CONTRACTOR		PROJECT NAME	REFERENCE DWG NO	JOB ORDER No	REPORT No	SHEET No
YIGITCAN ATILGAN		TEST PARÇALARI		5 EBRULUHAZIR	DFY0347/001	1 OF 1
EQUIPMENT/LINE No		INSPECTION PROCEDURE	TEST SPECIFICATION	ACCEPTANCE CRITERIA		
D02001/001/01		RS EN ISO 17634-1	TS EN ISO 17634-1	TS EN ISO 18275-1		
MATERIAL TYPE / WALL THICKNESS		TEST PLACE / TEST ITEM		CORRUPTION		
A36		A36		C02 / 12MM		
WELD STRUCTURE DATE		FILLER MATERIAL				
ELECTRIC WELD		E0303				
WELDING PROCESS		SMW (131)	GTAW (141)	SMW (131)	SAW (101)	OTHERS
KAYNAK YÖNTEMİ		Elektrodlü	Yak	Elektrodlü	Yak	Diğerler
JOINT DESIGN		WELD	MACHINED	GROUND	CAST	ROLLED
BİRLİKLE KULLANILAN		Yak	Elektrodlü	Elektrodlü	Elektrodlü	Elektrodlü
SURFACE CONDITION		BEFORE HEAT TREATED	AFTER HEAT TREATED	PREPARED EDGE	AFTER HYDROTEST	MACHINING TEST SURFACE
YÜZ YAPISI		Elektrodlü	Elektrodlü	Elektrodlü	Elektrodlü	Elektrodlü
STAGE OF EXAMINATION		AS WELDED	AFTER 1st LAYER	PREPARED EDGE	AFTER HYDROTEST	MACHINING TEST SURFACE
KONTROL YERİ		Elektrodlü	Elektrodlü	Elektrodlü	Elektrodlü	Elektrodlü
WELD STRUCTURE DATE		AS WELDED	AFTER 1st LAYER	PREPARED EDGE	AFTER HYDROTEST	MACHINING TEST SURFACE
ELEKTRİK WELD		Elektrodlü	Elektrodlü	Elektrodlü	Elektrodlü	Elektrodlü
EQUIPMENT / CHAZ		XRAY	SA	KVP	EXPOSURE TIME	EXPOSURE TIME
KULLANILAN EKİPMAN		Elektrodlü	Elektrodlü	Elektrodlü	Elektrodlü	Elektrodlü
SHOT PARAMETERS / ÇEKİM PARAMETRELERİ		PANORAMİK FANARÇLIK	DOUBLE WALL/DOUBLE IMAGE	DOUBLE WALL/DOUBLE IMAGE	DOUBLE WALL/DOUBLE IMAGE	DOUBLE WALL/DOUBLE IMAGE
ÇEKİM YERİ		Elektrodlü	Elektrodlü	Elektrodlü	Elektrodlü	Elektrodlü
FILM / FILM		KODAK	AGFA	FLUO	OTHERS	OTHERS
KULLANILAN FILM		Elektrodlü	Elektrodlü	Elektrodlü	Elektrodlü	Elektrodlü
WELD NO EXTENSIVE		REPAIR	REWORK	EX	EXTENSIVE	EXTENSIVE
KONTROL YERİ		Elektrodlü	Elektrodlü	Elektrodlü	Elektrodlü	Elektrodlü
FILM EXPOSURE TIME		EXPOSURE TIME	EXPOSURE TIME	EXPOSURE TIME	EXPOSURE TIME	EXPOSURE TIME
KULLANILAN FILM		Elektrodlü	Elektrodlü	Elektrodlü	Elektrodlü	Elektrodlü
TYPES OF DEFECT / HATA TİPLERİ		Porosity	Slag Inclusion	Crack	Undercut	Spatter
KULLANILAN FILM		Elektrodlü	Elektrodlü	Elektrodlü	Elektrodlü	Elektrodlü

Figure 9. Radiographic examination report

### 3.2. Destructive Testing

#### 3.2.1. Macrostructure studies

Macroscopic examination, cross-sectional macro images (Figure 10) of the plates joined by welding according to TS EN ISO 17639 standard were examined. When the macrostructure photographs were examined, it was determined that the single-pass welding of the sample joined at 450 A did not penetrate the root pass and a melting/penetration defect of approximately 2 mm in diameter occurred. Additionally, it was determined that a melting/penetration deficiency of approximately 0.5 mm in diameter occurred in the sample joined at 475 A. No welding mistakes were observed in the samples joined at other welding currents. Additionally, the weld metal and base material are clearly distinguished in the macrostructure images. In addition, it was seen from the images that single-pass welding and root pass processes were performed in all the samples combined with different welding currents. Additionally, it was determined that there was no symmetry error in the weld pass and root pass processes and no sagging occurred in the root pass. As a result of the macrostructure examinations of pressure vessel steels joined by the submerged arc welding method, it has been reported that no welding defects were encountered in the welding zone of the joints [18,19].

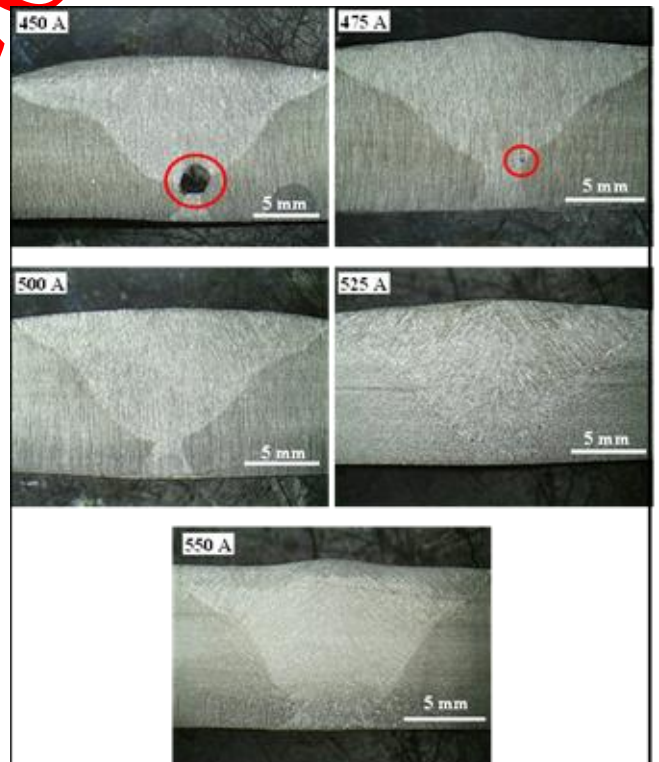


Figure 10. Macrostructure images

### 3.2.2. Microstructure studies

Microstructure images of plates welded with submerged arc welding using different welding currents are given in Figures 11-15. When the microstructure images were examined, similar structures were seen at the HAZ, weld metal and melting line boundaries of the plates joined

using different welding currents. It was observed that the HAZ grain sizes became slightly larger due to the increasing heat input as the welding current increased. In the images, the white grains have a ferritic structure and the black grains have a pearlitic structure. Moreover, pre-eutectoid ferrite and widmanstätten structures were also detected in the weld metal.

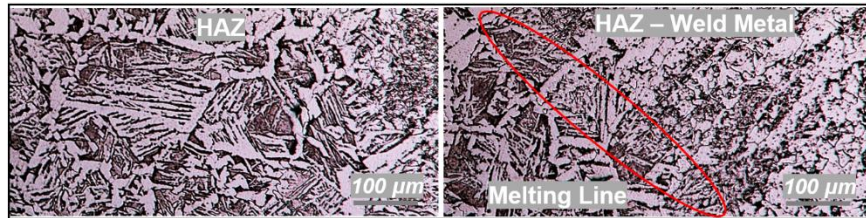


Figure 11. Microstructure of the plate combined at 450 A welding current

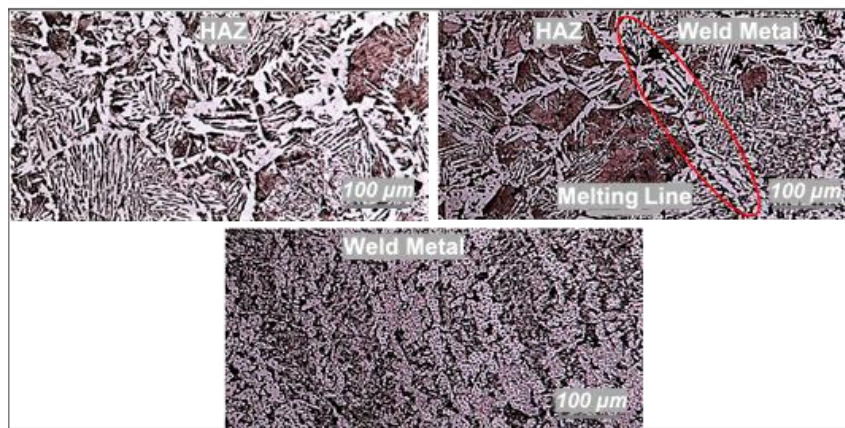


Figure 12. Microstructure of the plate combined at 475 A welding current

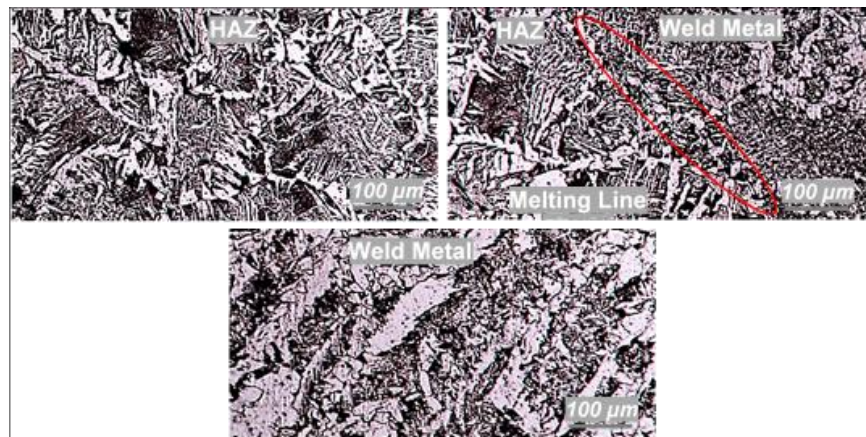
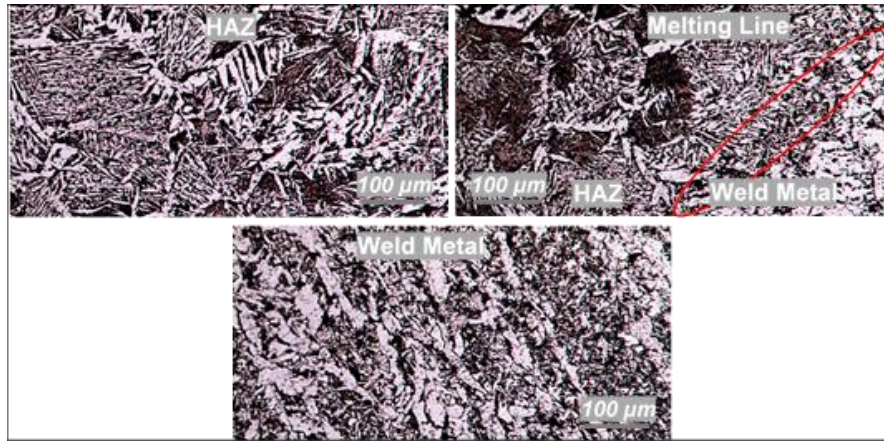
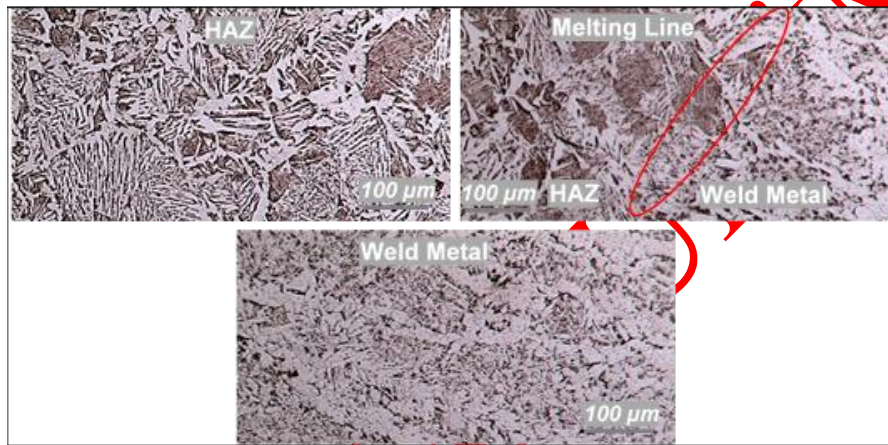


Figure 13. Microstructure of the plate combined at 500 A welding current



**Figure 14.** Microstructure of the plate combined at 525 A welding current



**Figure 15.** Microstructure of the plate combined at 550 A welding current

When the images are evaluated in general, it is observed that the grains in the HAZ become larger, whilst in the weld metal the grains have a columnar structure and extend in the direction of heat flow (towards the base material). Eroğlu and Aksoy [20] investigated the effects of heat input change on microstructure/mechanical properties in welded joints. According to microstructure examinations, it was stated that high heat input slows down cooling and solidification and causes more grain coarsening. It was also observed that the weld metal is made up of large and columnar grains, which are directed towards the centre of the weld metal. The microstructures of ship plates of different thicknesses joined by submerged arc welding method were examined. As a result of the investigations, it has been reported that grain boundary ferrite, widmanstätten ferrite, acicular ferrite, pearlite and martensite structures may form in the weld metal of low carbon and low alloy steels, depending on the cooling rate. Additionally, as a result of microstructural studies, it was stated that it consists mainly of acicular ferrite and polygonal ferrite structures [21].

### 3.2.3. Hardness test

The graph obtained because of the hardness tests applied horizontally to the welding zone of the plates

joined by the submerged arc welding method is given in Figure 16.

When the microhardness results of the joints made using different welding currents was explored, it was observed that the measured hardness values were close to each other, but the samples joined using 550 A welding current had higher hardness values. It is thought that the increase in hardness values due to the increase in current values is due to heat input. It was determined that the hardness values of the weld metal in all samples were higher than the HAZ and the base material. The highest hardness value was determined in the weld metal, followed by HAZ and base material. The difference in hardness values of weld metal, HAZ and base material varies depending on the heat and cooling rate they are exposed to. It is thought that the increasing Mn ratio in the chemical composition of the additional wire and welding flux used may be effective as the reason why the hardness of the weld metal is higher than that of the HAZ and the base material.

Weld metal hardness values were measured as (450 A)  $200 \pm 5$  HV, (475 A)  $202 \pm 5$  HV, (500 A)  $203 \pm 5$  HV, (525 A)  $205 \pm 5$  HV, and (550 A)  $207 \pm 5$  HV. HAZ hardness values were measured as (450 A)  $185 \pm 5$  HV, (475 A)  $186 \pm 5$  HV, (500 A)  $188 \pm 5$  HV, (525 A)  $190 \pm 5$  HV, and (550 A)  $191 \pm 5$  HV. The hardness value of the base

material was measured as  $160 \pm 5$  HV. In hardness measurements of steel joints previously made by submerged arc welding [22-25], the highest value was determined the weld metal. It has been stated that there is a decrease in hardness values as one moves towards the base material.

( $567 \pm 5$  N/mm<sup>2</sup>), respectively. These values were found to be higher than the tensile strength of the base material (528 N/mm<sup>2</sup>). The reason why the samples joined in these welding currents show higher tensile strength can be explained by the fact that the hardness values of the weld metal and HAZ (Figure 16) are higher than the base

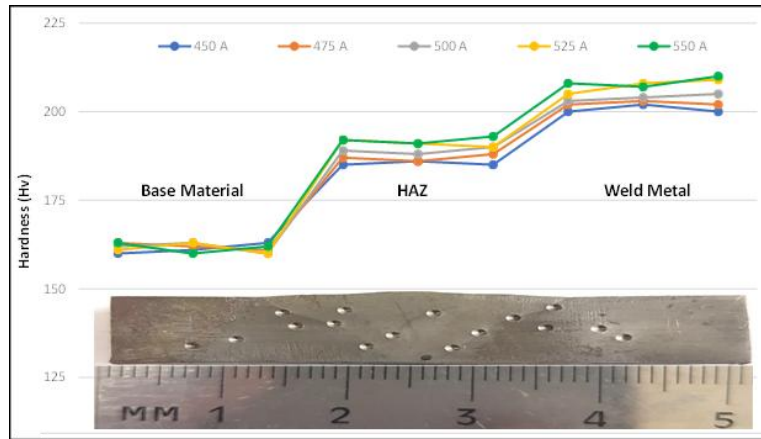


Figure 16. Hardness test results

### 3.2.4. Tensile test

The graph of the tensile tests applied to the sheets joined using the submerged arc welding method is given in Figure 17, and the rupture images after the tests are given in Figure 18.

When the tensile test results were examined, the rupture occurred in the welding zone in the plates joined to 450 A and 475 A, while the rupture occurred in the base material in the plates joined to 500 A, 525 A and 550 A. It was determined that the tensile strength of the sheets joined at 450 A ( $435 \pm 5$  N/mm<sup>2</sup>) and 475 A ( $458 \pm 5$  N/mm<sup>2</sup>) welding currents was lower than the tensile strength of the base material (528 N/mm<sup>2</sup>). Ultrasonic (Figure 7), radiographic (Figure 8-9) and macrostructure (Figure 10) results showed that 450 A and 475 A values were not appropriate. In the sample joined at 450 A welding current, it was observed that the welding performed in a single pass did not penetrate the root pass and a lack of melting/penetration occurred with a diameter of approximately 2 mm. It was observed that there was a melting/penetration deficiency of approximately 0.5 mm in the sample joined at 475 A welding current. Tensile test results confirm the results of non-destructive testing and macrostructure studies.

The tensile strengths of the welding areas of the plates joined at 500 A, 525 A and 550 A welding current were determined as ( $541 \pm 5$  N/mm<sup>2</sup>), ( $552 \pm 5$  N/mm<sup>2</sup>) and

material due to the increasing heat input (Table 3) in parallel with the increase in the welding current. Similarly, according to the previous analysis results, the results of the non-destructive and macrostructure studies did not indicate that any welding defects were found in the welding area, and the tensile test results were also supported by these results. The samples that broke in the weld area after the tensile test broke brittle due to the welding defects mentioned above. However, the samples that fractured in the base material experienced ductile failure, and the weld zone did not show any visible damage. In the samples united at 500 A, 525 A or 550 A, the rupture zones were observed in the base material, not in the weld metal or HAZ.

In addition, samples welded at 450 A and 475 A showed 8.4 and 9.3% elongation in tensile tests due to the welding errors mentioned above. While the % elongation of the base material was 22%, the samples joined at 500 A, 525 A and 550 A exhibited % elongation of 21.2%, 19.7% and 18.6%, respectively. The reason why these samples exhibit less % elongation than the base material can be explained by the fact that the hardness values of the weld metal and HAZ are higher than the base material due to the increasing heat input in parallel with the increase in welding current (Figure 16). Similar results have been reported after tensile tests applied to steels joined by submerged arc welding method [19,26,27].

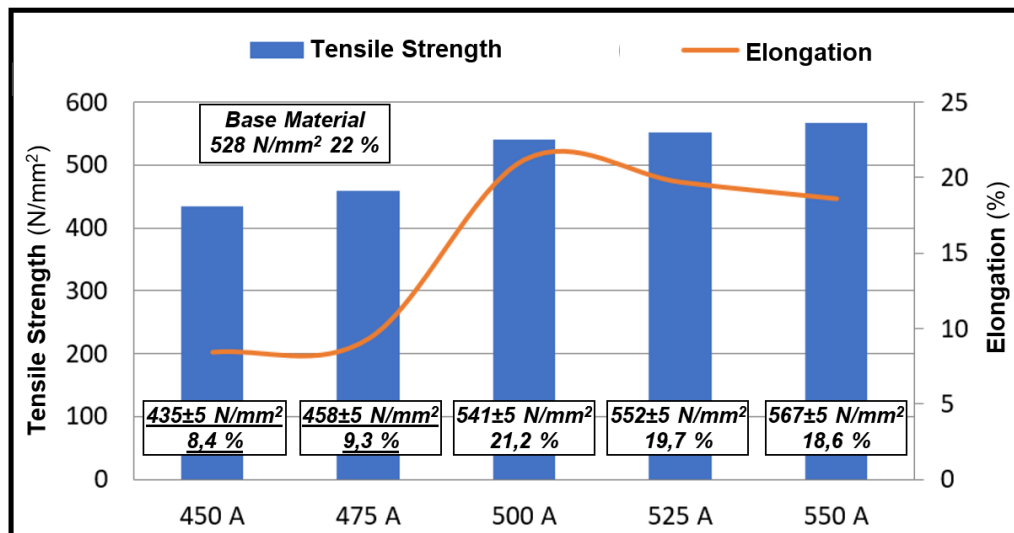


Figure 17. Tensile and elongation graph

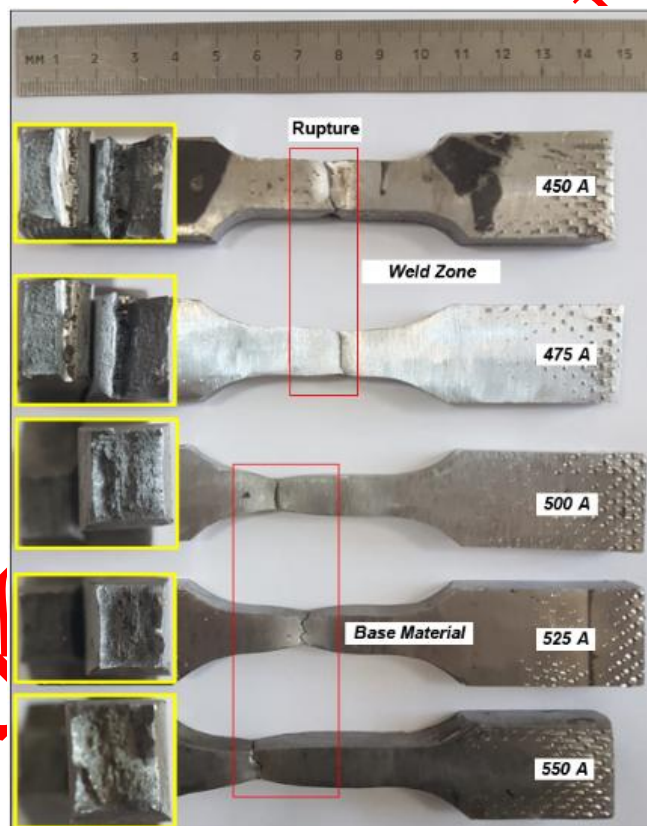


Figure 18. Fracture images after tensile test

### 3.2.5. Bending test

Sample images after the 180° bending test applied to welded samples are given in Figure 19. When the sample images were examined after the bending test, cracking and tearing occurred in the welding zones of the samples joined using 450 A and 475 A. However, no welding defects were observed in the samples joined using 500 A, 525 A and 550 A. These results also coincide with the non-destructive tests and macrostructure studies applied to the samples in the previous sections.

As a result, it has been determined that the samples joined at 450 A and 475 A using the submerged arc welding method are not suitable for use by bending, while the samples joined at 500 A, 525 A and 550 A welding current can be used by bending under service conditions. As a result of bending tests applied to different materials joined using the submerged arc welding method, it was reported that no visible damage occurred in the samples when appropriate welding parameters were used [28,29].

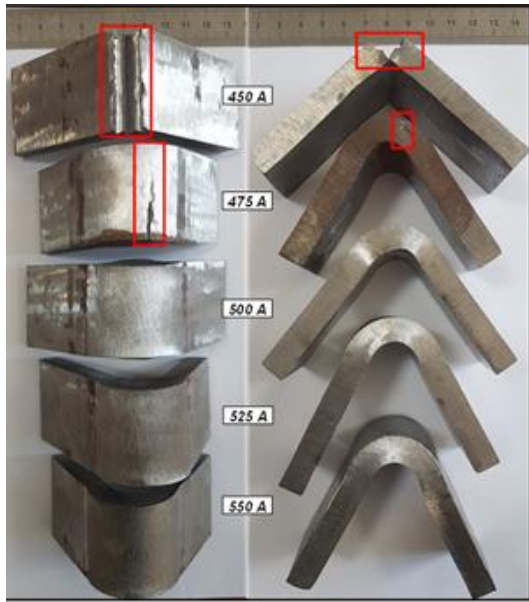


Figure 19. Images of the sample after the bending test

### 3.2.6. Notch impact test

Notch impact tests were conducted to ascertain the impact toughness of the sheets joined via the submerged arc welding method, the weld metal and HAZ at temperatures of -20 oC, 0 oC, and 20 oC. Figure 20 indicates the weld metal, while Figure 21 illustrates the HAZ's impact toughness.

When the impact toughness graphs were investigated, it was seen that the highest toughness was obtained at the test temperature of 20°C (room temperature), followed by the test temperatures of 0°C and -20°C, respectively. It was determined that as the test temperatures decreased, the impact toughness of the welded samples also decreased. It has been reported that after notch impact tests applied to steels joined by submerged arc welding method, impact toughness decreases with decreasing test temperature [15-17,28].

When weld metal impact toughness is examined, it is seen that there is a significant decrease in the samples joined at 450 A and 475 A. The reason for this decrease, as stated in the previous sections, is the lack of penetration at the root in the samples combined with these welding currents. Results inversely proportional to hardness were determined in the samples joined at 500 A, 525 A and 550 A. HAZ impact toughness was similarly found to be inversely proportional to the hardness results. When weld metal and HAZ impact toughness's are compared, it is seen that HAZ impact toughness's are higher than weld metal toughness's. When the impact toughness was compared with the hardness test results, it was determined that the toughness values decreased as the hardness increased. In a study, it was reported that as hardness values increased, toughness values decreased [30].

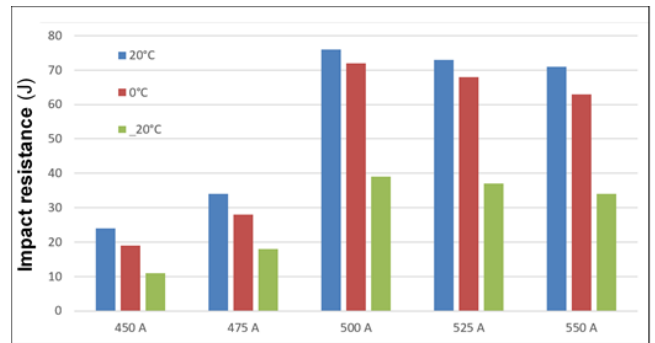


Figure 20. Weld metal impact toughness chart

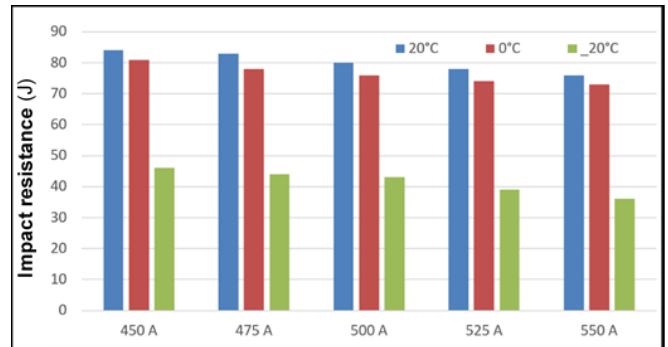


Figure 21. HAZ impact toughness chart

## 4. CONCLUSIONS

- No discontinuity was observed on the weld surfaces in liquid penetrant and magnetic particle tests.
- In ultrasonic examinations, a lack of root penetration was observed in the sheets joined using 450 A and 475 A. No discontinuity was observed in the plates joined using 500 A, 525 A and 550 A.
- As a result of ultrasonic examination, lack of penetration at the root (insufficient penetration) was observed in the plates welded at 450 A and 475 A. No discontinuities (undercut, residue, pores, cracks, etc.) were observed in the plates joined at 500 A, 525 A and 550 A.
- As a result of macrostructural examinations, it was observed that there was melting/penetration insufficiency in the samples joined at 450 A and 475 A welding current. No welding defects were detected in the welding area of the samples joined using other welding currents.
- In the microstructure images, it was observed that the grains became larger in the HAZ, while the grains in the weld metal had a columnar structure and extended in the direction of heat flow (towards the base material).
- When the hardness values were examined, the highest hardness values in all samples were obtained from the weld metal, followed by HAZ and the base material, respectively.
- While the rupture occurred in the welding zone in the plates welded using 450 and 475A in the tensile tests, the rupture occurred in the base

material in the samples combined with other welding currents.

- In bending tests, cracking and tearing are observed in the welding zones of the samples joined using 450 and 475A, while there is no cracking, tearing, etc. in the samples joined using other welding currents. No welding errors were found.
- As a result of the notch impact tests, it was determined that the highest toughness values were obtained at the test temperature of 20°C (room temperature), followed by the test temperatures of 0°C and -20°C, respectively.

## DECLARATION OF ETHICAL STANDARDS

The authors of this article declare that the materials and methods used in this study do not require ethical committee permission and/or legal-special permission

## AUTHORS' CONTRIBUTIONS

**Yiğitcan ATILGAN:** Performed the experiments.

**Mehmet Serkan YILDIRIM:** Analyzed the results and wrote the manuscript.

**Yakup KAYA:** Analyzed the results.

## CONFLICT OF INTEREST

There is no conflict of interest in this study.

## REFERENCES

- [1] Internet A: [https://en.wikipedia.org/wiki/A36\\_steel](https://en.wikipedia.org/wiki/A36_steel) (2012).
- [2] Atılğan Y., “Depolama tankı imalatında tozaltı ark kaynağı uygulaması ve kaynak bölgesinin incelenmesi”, *Master's Thesis*, Karabük University Institute of Science and Technology, Karabük, 1-71, (2022).
- [3] Marquez-Herrera A., Saldana-Robles A., Zapata-Torres M., Reveles-Arredondo J.F. and Diosdado-De la Pena J.A., “Duplex surface treatment on ASTM A-36 steel by slide burnishing and powder pack boriding”, *Materials Today Communications*, 31, (2022).
- [4] Márquez-Herrera A., Fernandez-Muñoz J.L., Zapata-Torres M., Melendez-Lira M. and Cruz-Alcantar P., “Fe<sub>2</sub>B coating on ASTM A-36 steel surfaces and its evaluation of hardness and corrosion resistance”, *Surface & Coatings Technology*, 254:433-439, (2014).
- [5] Çetinkaya C., Taşçı S. and Ada H., 3Cr12 Ferritik Paslanmaz Çeliklerin Gaz Metal Ark Kaynağıyla Birleştirilmesinde İlave Tel Türünün Mikroyapı ve Mekanik Özelliklere Etkisinin Araştırılması”, *Journal of Polytechnic*, 26(4): 1651-1660, (2023).
- [6] Çetinkaya C., Akay A. and Özdemir U., “A comparative investigation into the impact of shop-primer coating on weldability of S235JR steel using MAG and SAW processes”, *Journal of Polytechnic*, 26(4): 1587-1600, (2023).
- [7] Yalçın F., Yıldırım M. S. ve Kaya Y., “Joining of pressure vessel steels using MAG welding method and investigation of mechanical properties”, *Journal of Polytechnic*, \*(\*) : \*, (\*).
- [8] Kaya Y., “An investigation of joinability of S235JR and S355JR construction steel by MAG welding method with cored wire electrode”, *Journal of Polytechnic*, 21(3): 597-602, (2018).
- [9] Harman M., Ada H. ve Çetinkaya C., “Determination of the effect of additional metal wire diameter on metallurgical and mechanical properties in TIG welding of QSTE 420TM steel”, *Journal of Polytechnic*, 23(3): 829-839, (2020)
- [10] Akhyar., Tamlicha A., Farhan A., Azwinur., Syukran., Fadhilah T. A., Firsat., Ghazilla R. A. R., “Evaluation of welding distortion and hardness in the A36 steel plate joints using different cooling media”, *Sustainability*, 14: 1405, (2022).
- [11] Eisazadeha H., Achuthana A., Goldakb J. A., Aiduna D. K., “Effect of material properties and mechanical tensioning load on residual stress formation in GTA 304-A36 dissimilar weld”, *Journal of Materials Processing Technology*, 222: 344-355, (2015).
- [12] Thirunavukkarasu K., Kavimani V., Gopal P. M., “Effect of recycled flux over mechanical properties of A36 steel in submerged arc welding”, *International Journal of Sustainable Engineering*, 14: (6) 1962-1970, (2021).
- [13] Sharma H., Rajput B., Singh R. P., “A review paper on effect of input welding process parameters on structure and properties of weld in submerged arc welding process”, *Materials Today: Proceedings*, 26: 1931-1935, (2020).
- [14] Özkan E., “Kaynak sonrası S355J2N yapı çeliğinde oluşan gerilmeleri gidermek için uygulanan ısıtma işleminin etkilerinin tahribatlı-tahribatsız muayene yöntemleriyle belirlenmesi”, *Master's Thesis*, Tekirdağ Namık Kemal University Institute of Science and Technology, Tekirdağ, 1-80, (2019).
- [15] Akay A., “Farklı özellikteki malzemelerin tozaltı ark kaynak yöntemi ile birleştirilmesi ve birleştirmelerin tahribatlı ve tahribatsız muayenesi”, *Master's Thesis*, Karabük University Institute of Science and Technology, Karabük, 1-99, (2012).
- [16] Akay A., Kaya Y., Kahraman N., “Farklı özellikteki malzemelerin tozaltı ark kaynak yöntemi ile birleştirilmesi ve birleştirmelerin tahribatlı ve tahribatsız muayenesi”, *Sakarya University Journal of Science*, 83-94, (2013).
- [17] Acar O., “Petrol depolama tanklarının imalatı montajı ve kaynaklı bağlantılarının tahribatsız muayenesi”, *Master's Thesis*, Sakarya University Institute of Science and Technology, Sakarya, 1-166, (2009).
- [18] Canlı A., “Östenitik paslanmaz çelik ve IF çeliğinin nokta direnç kaynak yöntemi ile birleştirilebilirliğinin incelenmesi”, *Master's Thesis*, Karabük University Institute of Science and Technology, Karabük, 1-78, (2017).
- [19] Canlı A., Yıldırım M. S., Kaya Y., “Tozaltı kaynak yöntemleriyle S355J2-P460 basınçlı kap çeliklerinin birleştirilebilirliğinin araştırılması” *2nd International Turkish World Engineering and Science Congress*, November 7-10, Turkey, 809-816, (2019).

- [20] Erođlu M., Aksoy M., “Enerji giriřinin kaynak metali mikroyapısı ve mekanik özellikleri üzerine etkisi”, *Science Days, Proceedings Book, Chamber of Mechanical Engineers*, Denizli, 434-439, (1999).
- [21] Kaya Y., Kahraman N., Durgutlu A., Gülenç B., “Tozaltı ark kaynađı ile birleřtirilen farklı kalınlıktaki grade A gemi saclarının mekanik özelliklerinin arařtırılması”, *e-Journal of New World Sciences Academy Engineering Sciences*, 1A0088, 5 (2): 348-357 (2010).
- [22] Kılınçer S., “Düşük karbonlu çeliklerin tozaltı ark kaynak yöntemi ile kaynak edilebilirliđinin ve mekanik özelliklerinin incelenmesi”, *Master's Thesis*, Gazi University Institute of Science and Technology, Ankara,12-22, (1998).
- [23] Durgutlu A., Kahraman N., Gülenç B., “Tozaltı ark kaynađında kaynak tozunun mikroyapı ve mekanik özelliklere etkisinin incelenmesi”, *The Journal of the Industrial Arts Education Faculty of Gazi University*, 10 (11): 1-8, (2002).
- [24] Ada H., “Petrol ve dođalgaz boru hatları için üretilen boruların Tozaltı ve spiral kaynak yöntemiyle kaynaklanabilirliđi ve mekanik özelliklerinin incelenmesi”, *Master's Thesis* Gazi University Institute of Science and Technology, Ankara,14-69, (2006).
- [25] Asarkaya M., “Gemi insasında kullanılan kaynak yöntemlerinin mekanik özelliklere etkisi”, *Master's Thesis*, Sakarya University Institute of Science and Technology, Sakarya, 54-86, (2006).
- [26] Kahraman N., Gülenç B. Durgutlu A., “Tozaltı ark kaynađı ile kaynaklanan düşük karbonlu çeliklerde serbest tel uzunluđunun mikroyapı ve mekanik özelliklere etkisinin arařtırılması”, *Gazi University Journal of Science*, 18 (3): 473-480, (2005).
- [27] Usta M., “Birbirinden farklı kalın cidarlı basınçlı kaplarda kaynaklı bölgelerin TS 17020 uygunluđunun arařtırılması”, *Master's Thesis*, Namık Kemal University Institute of Science and Technology, Tekirdađ,1-52, (2011).
- [28] Kurt K., “DH 36 gemi sacının farklı kaynak yöntemleri ile mekanik özelliklerinin incelenmesi”, *Master's Thesis*, Sakarya University Institute of Science and Technology, Sakarya,1-89, (2008).
- [29] Kaya Y., Canlı A., “Tozaltı ark kaynak yöntemiyle birleřtirilen basınçlı kap çeliklerinin mikroyapı ve mekanik özelliklerinin incelenmesi” *IV. International Symposium on Multidisciplinary Studies (ISMS)*, Paris/France 27-28 April, 67-78, (2018).
- [30] Çetinkaya C., “Düşük karbonlu çeliklerin tozaltı ark kaynak yöntemi ile kaynak edilebilirliđi ve mekanik özelliklerinin incelenmesi”, *Gazi University Journal of Science*, 12 (2): 279-293, (1999).